HHS Public Access

Author manuscript

Hum Mutat. Author manuscript; available in PMC 2016 May 01.

Published in final edited form as:

Hum Mutat. 2015 November ; 36(11): 1021–1028. doi:10.1002/humu.22828.

WDR73 mutations cause infantile neurodegeneration and variable glomerular kidney disease

Julia Vodopiutz[1], **Rainer Seidl**[1], **Daniela Prayer**[2], **M. Imran Khan**[3], **Johannes A. Mayr**[4], **Berthold Streubel**[5], **Jens-Oliver Steiß**[6], **Andreas Hahn**[7], **Dagmar Csaicsich**[1], **Christel Castro**[8,9], **Mirna Assoum**[8,9], **Thomas Müller**[3], **Dagmar Wieczorek**[10], **Grazia M. S. Mancini**[11], **Carolin E. Sadowski**[12,13], **Nicolas Levy**[8,9,14], **André Mégarbané**[15,16], **Koumudi Godbole**[17], **Denny Schanze**[18], **Friedhelm Hildebrandt**[12], **Valérie Delague**[8,9,*], **Andreas R. Janecke, MD**[3,19,*], and **Martin Zenker**[18,20,*]

[1]Department of Pediatrics and Adolescent Medicine, Medical University of Vienna, Austria [2]Division of Neuroradiology and Musculoskeletal Radiology, Medical University of Vienna, Austria [3]Department of Pediatrics I, Medical University of Innsbruck, Innsbruck, Austria [4]Department of Pediatrics, Paracelsus Medical University, Salzburg, Austria [5]Department of Obstetrics and Feto-Maternal Medicine, Medical University of Vienna, Austria [6]Department of Pediatrics, Justus-Liebig-University, Gießen, Germany [7]Department of Child Neurology, Justus-Liebig-University, Gießen, Germany [8]Inserm, UMR_S 910, 13385, Marseille, France [9]Aix Marseille Université, GMGF, 13385, Marseille, France [10]Institute of Human Genetics, University of Essen, Germany [11]Department of Clinical Genetics, Erasmus University Medical Center, Rotterdam, The Netherlands [12]Harvard Medical School, Boston Children's Hospital, Boston, Massachusetts, USA [13]Department of Gynecology and Obstetrics, University Hospital Carl Gustav Carus, Technische Universität Dresden, Germany [14]Département de Génétique Médicale, Hôpital d'Enfants de la Timone, AP-HM, Marseille, France [15]Université Saint Joseph, Campus des Sciences Médicales, Unité de génétique médicale, Lebanon [16]Institut Jérôme Lejeune, Paris, France [17]Deenanath Mangeshkar Hospital & Research Center, Erandawane, Pune, India [18]Institute of Human Genetics, University Hospital, Magdeburg, Germany [19]Division of Human Genetics, Medical University of Innsbruck, Innsbruck, Austria [20]Institute of Human Genetics, University of Erlangen, Erlangen, Germany

Abstract

Infantile-onset cerebellar atrophy (CA) is a clinically and genetically heterogeneous trait. Galloway-Mowat syndrome (GMS) is a rare autosomal recessive disease, characterized by microcephaly with brain anomalies including CA in some cases, intellectual disability, and early-infantile-onset nephrotic syndrome. Very recently, WDR73 deficiency was identified as the cause

Correspondence: Prof. Dr. med. Martin Zenker, Institute of Human Genetics, University Hospital, Leipziger Str. 44, 39120 Magdeburg, Germany, Phone: +49 391 6715064, Fax: +49 391 6715066, martin.zenker@med.ovgu.de. Dr. med. Andreas R. Janecke, Department of Pediatrics I and Division of Human Genetics, Medical University of Innsbruck, Anichstrasse 35, A-6020 Innsbruck, Austria, Phone: +43 512 504 26345, Fax: +43 512 504 24525, andreas.janecke@i-med.ac.at.

*These authors contributed equally to this work.

SUPPLEMENTAL MATERIAL

This article refers to a Supplemental Material and Results file.

of GMS in five individuals. To evaluate the role of *WDR73* mutations as a cause of GMS and other forms of syndromic CA, we performed Sanger or exome sequencing in 51 unrelated patients with CA and variable brain anomalies and in 40 unrelated patients with a diagnosis of GMS. We identified 10 patients from three CA and from two GMS families with *WDR73* mutations including the original family described with CA, mental retardation, optic atrophy and skin abnormalities (CAMOS). There were five novel mutations, of which two were truncating and three were missense mutations affecting highly conserved residues. Individuals carrying homozygous *WDR73* mutations mainly presented with a pattern of neurological and neuroimaging findings as well as intellectual disability, while kidney involvement was variable. We document postnatal onset of CA, a retinopathy, basal ganglia degeneration, and short stature as novel features of WDR73-related disease, and define WDR73-related disease as a new entity of infantile neurodegeneration.

Keywords

Neurodegeneration; cerebellar atrophy; basal ganglia; intellectual disability; optic atrophy; short stature; retinopathy; WDR73; recessive; Galloway-Mowat syndrome; CAMOS; SCAR5; exome sequencing

INTRODUCTION

Cerebellar atrophy (CA) is an unspecific neuroradiological sign defined as a cerebellum with normally developed architecture but enlarged interfolial spaces in a normal fossa posterior. CA with infantile onset can be isolated or part of a syndrome and occurs in hereditary ataxias, neurodegenerative or metabolic disorders, PEHO syndrome (MIM #260565), and in other conditions (Wolf and Koenig, 2013). Ataxia is the major clinical symptom of CA and the mode of inheritance in CA with infantile onset is generally autosomal recessive. As a large number of monogenic causes are known to cause infantile onset CA, it is a common problem to make a definitive molecular diagnosis in these patients. Galloway-Mowat syndrome (GMS; MIM #251300) is a rare autosomal recessive disease, which is characterized by microcephaly with brain anomalies including CA in some cases, intellectual disability, epilepsy and early-infantile-onset nephrotic syndrome. GMS is clinically heterogeneous (Galloway and Mowat, 1968; Cooperstone et al., 1993; Steiss et al., 2005; Dietrich et al., 2008). Very recently, WDR73 (MIM #616144) deficiency was identified in five individuals with GMS presenting with childhood-onset nephrotic syndrome, postnatal microcephaly, severe intellectual disability, and homogenous brain MRI features including CA (Colin et al., 2014; Ben-Omran et al., 2015).

WDR73 encodes a protein predicted to contain six 40–60 amino acid WD40 repeats. A WD40 repeat folds into a four-stranded antiparallel beta-sheet blade, and such blades often assemble into domains containing a seven-bladed propeller called the WD40 domain. These domains act as platforms for protein assembly, making them hubs in many cell-signaling networks (Stirnimann et al., 2010). Immunohistochemistry experiments performed on human tissue samples, showed that WDR73 was expressed in renal glomeruli and in infant and adult brain, where immunostaining was particularly strong in Purkinje cells and their

projecting axons in cerebellum, the deep cerebellar nuclei, and pyramidal neurons of cerebral cortex. It was suggested, that WDR73 plays a role in cell survival and microtubule regulation (Colin et al., 2014).

In this study, we investigated a large cohort of patients with CA and variable additional brain anomalies and a large cohort of patients with GMS for *WDR73* mutations. We show here that biallelic WDR73 mutations are associated with a much broader phenotypic spectrum than previously described, characterized mainly by its neurological features with minor or even no kidney involvement.

MATERIALS AND METHODS

Patients

We studied at total of 91 unrelated families with 110 affected individuals; there were 51 unrelated families with 58 patients affected by CA and variable brain anomalies and 40 unrelated families with 52 patients affected by GMS. Patients were not included if autosomal dominant inheritance was suggested. Each patient was seen by a child neurologist and had a standardized neurological assessment. DNA was sampled from all patients and available family members. Family history, medical reports, and brain MRIs were collected. The CA cohort included a family previously reported with CAMOS syndrome (Cerebellar Ataxia with Mental Retardation, Optic Atrophy and Skin Abnormalities) (Megarbane et al., 2001), alternatively named SCAR5 (spinocerebellar atrophy, autosomal recessive, type 5; MIM #606737).

Approvals and patient consents

Written informed consent was obtained from all patients or their legal representative for genetic analysis. Family 1 was recruited at Medical University of Vienna and included in a study, which was approved by the local ethics committee. Cohorts of patients for *WDR73* sequencing were recruited by the Medical University of Vienna, Innsbruck Medical University, University Hospital of Erlangen, Saint-Joseph University (Beirut, Lebanon), UMR_S 910 at Inserm/Aix Marseille University (Marseille, France) and the Erasmus University Medical Center (Rotterdam, The Netherlands) and included in studies, which were approved by these local ethics committees.

Genetic analyses

Linkage analysis and exome sequencing—In the consanguineous family 1, genetic linkage analysis and exome sequencing were performed; DNA samples from five family members were genotyped with Genome-Wide Human SNP Array 6.0 (Affymetrix) arrays, genotypes were called with Genotyping Console (Affymetrix), and linkage files were prepared using the Alohomora program (http://gmc.mdc-berlin.de/alohomora/) with the “select markers for linkage option” set to a minimal distance between adjacent markers of 50 Kb and a minor allele frequency set to ≥ 0.15. Multipoint likelihood-of-the-odds (LOD) scores were obtained with the Merlin program (Abecasis et al., 2002) under the hypothesis of an autosomal-recessive, fully penetrant mutation, inherited identical-by-descent. Exome sequencing of patient II-1 from family 1 was performed using Roche-Nimblegen’s SeqCap

EZ Exome v2 kit on an Illumina HiSeq2000. Paired-end reads were aligned to the human reference genome with Burrows-Wheeler transformation (Li and Durbin, 2009). Polymerase chain reaction (PCR) duplicates were removed with PICARD (http://picard.sourceforge.net) and single nucleotide substitutions, and small indels were called with SAMtools software. All variants were submitted to SeattleSeq (http://snp.gs.washington.edu/SeattleSeqAnnotation/) for annotation, categorization, and filtering for allele frequencies in public variant databases dbSNP138, the 1000 Genomes Project, the National Heart, Lung, and Blood Institute (NHLBI) Exome Sequencing Project (ESP). The exome aggregation consortium server (EXAC, exac.broadinstitute.org) was manually searched for allele frequencies of identified *WDR73* variants. All of the variants with minor allele frequency of >5% in the 1000 genomes or in the ESP database were discarded in order to remove common polymorphism and sequencing artefacts.

***WDR73* mutation screening by exome sequencing—**The WDR73 gene was analyzed by exome sequencing in further 19 unrelated patients (two patients with CA and variable brain anomalies and 17 patients with GMS) on lymphocyte DNA was performed as described above, and covered the complete coding region and splice-sites of *WDR73*.

***WDR73* mutation screening by Sanger sequencing—**71 unrelated patients (48 patients with CA and variable brain anomalies and 23 patients with GMS) were screened for mutations in *WDR73* by PCR amplification and direct Sanger sequencing of the *WDR73* coding region and splice sites (National Center for Biotechnology Information (NCBI) reference sequence NM_032856.3), in which the A of the ATG translation initiation codon was nucleotide 1. Primers and conditions are provided in Supp. Table S1. Mutations were submitted to the Leiden Open Variation Database for WDR73 (http://databases.lovd.nl/shared/genes/WDR73). Of the 48 patients with CA and variable brain anomalies, 39 had had the ZNF592 gene sequenced and no biallelic or novel mutations had been found.

***WDR73* mutation segregation analyses—**Where genetic variations in *WDR73* were identified in patients, DNA of available family members was tested by Sanger sequencing for the presence of mutations identified in index patients with biallelic *WDR73* mutations, and segregation of mutations according to autosomal recessive inheritance was evaluated.

Amino acid conservation, in-silico analyses of mutational effect, and homology modeling—A set of protein reference sequences of WDR73 orthologues obtained from the NCBI database (http://www.ncbi.nlm.nih.gov/gene/?term=wdr73) was aligned using ClustalOmega and the effect of amino acid substitution on the function of WDR73 was assessed by in silico tools Polymorphism Phenotyping version 2 (PolyPhen-2, http://genetics.bwh.harvard.edu/pph/) (Adzhubei et al., 2010) with these options: Classifier model [HumDiv], Genome aseembly [GRCh37/hg19], Transcripts [CCDS], Annotations [All], Sorting Intolerant from Tolerant (SIFT, http://sift.jcvi.org/) (Ng and Henikoff, 2001) and UMD-Predictor (http://umd-predictor.eu/). The effects of identified missense mutations on WDR73 protein structure were modeled by two approaches: 1) I-TASSER modeling (http://zhanglab.ccmb.med.umich.edu/I-TASSER/) (Roy et al., 2010) and PyMol (Schrödinger, Portland, USA) visualization, and 2) modeling on PDB entries 3GFC and

1V9P, which were identified by BLASTP searches with WDR73 reference sequence NP_116245.2 (for details see Supp. Methods).

RESULTS

Identification of *WDR73* mutations in a cohort of patients with CA and variable brain anomalies

Combination of homozygosity mapping and exome sequencing was applied in family 1 (Table 1, Fig. 1) in order to identify the disease-causing gene for an unknown infantile neurodegenerative disease with CA in two siblings. Homozygosity mapping revealed a single, 11.2-Mb chromosomal candidate interval on chromosome 15 with the maximal obtainable LOD score of 1.9 in this family. This candidate region harbored a single novel or rare sequence variant in the proband's exome, a homozygous 2-basepair deletion in *WDR73* resulting in a premature termination codon (c.400_401delAG, p.(Trp136Alafs*2)) (Fig. 1). Exome sequencing did not reveal additional rare or private homozygous or compound heterozygous gene mutations in this proband exome-wide.

As CAMOS/SCAR5 had been mapped to an overlapping chromosomal region on chromosome 15 (Table 1, Fig. 1D) in the original Lebanese family (Delague et al., 2002) and presents with a similar neurological phenotype (Megarbane et al., 2001), we sequenced *WDR73* in this family and identified a homozygous *WDR73* mutation (c.1039C>T, p.(His347Tyr)) in all five affected individuals of this family (denoted family 2 in Table 1 and Fig. 1). This missense change affects an evolutionary highly conserved amino acid within the last of the six predicted WD40 domains of WDR73 (Table 1, Fig. 1C, 1D, Supp. Figures S1, S2). It was absent from 256 Lebanese control chromosomes and is listed as very rare in the EXAC database with 1 of 84,686 alleles bearing this mutation (allele frequency 0.00001181), altogether implying this mutation as underlying CAMOS/SCAR5 in this family, where a rare c.3136G>A (p.(Gly1046Arg), rs150829393) variant (EXAC database allele frequency 17/121372) in the neighboring gene *ZNF592* had previously been found to segregate with the disease and proposed as the causative genetic alteration (Nicolas et al., 2010).

We subsequently analyzed additional 49 unrelated patients with the clinical diagnoses of early-onset CA with and without variable brain anomalies via exome or Sanger sequencing of *WDR73*. This revealed one additional individual from an unrelated family carrying a homozygous *WDR73* variant, p.(Leu23Gln) (family 5 in Table 1, Fig. 1). *WDR73* was located within a 19 Mb region of homozygosity, the largest homozygous region revealed by high-resolution microarray genotyping in this individual (data not shown).

Identification of *WDR73* mutations in a cohort of patients with GMS

As WDR73 deficiency has been recently reported as the molecular cause in a subset of individuals with GMS, we also screened 40 unrelated individuals with the clinical diagnosis of GMS for *WDR73* mutations either by exome sequencing or by Sanger sequencing. This identified two additional individuals from two unrelated families carrying biallelic *WDR73* variants predicted to be damaging: a homozygous truncating c.940C>T (p.(Gln314*))

mutation was identified in a patient whose clinical phenotype has been published previously (Steiss et al., 2005); and a homozygous c.287G>A (p.(Arg96Lys)) missense mutation was identified in an unpublished patient with GMS (families 4 and 3 in Table 1, Fig. 1). Including affected siblings, we identified homozygous *WDR73* germline mutations in a total of 10 individuals from five families (Table 1, Fig. 1). Five different and novel *WDR73* mutations were found in these families. These mutations segregated with the disease in each family, as all parents of patients were heterozygous mutation carriers. In families 3 and 4 additional similarly affected siblings have been reported (Table 1, Fig. 1A) but neither a detailed documentation of the clinical and neurological phenotype nor DNA samples for molecular confirmation of *WDR73* mutations were available from these individuals. These results determine a detection rate of biallelic *WDR73* mutations of 3 of 51 (5.9 %) in our cohort of patients with CA and variable brain anomalies and of 2 of 40 (5 %) in our cohort of patients with GMS. The *WDR73* variants comprised one frameshift, one nonsense, and three presumably deleterious missense changes (Table 1, Fig. 1B–D). All five mutations are either private or very rare with respect to public sequence variant databases (Table 1), a first indication that they might be underlying the disease. The frameshift mutation p.(Trp136Alafs*2) generates an early termination codon and is predicted to undergo nonsense-mediated RNA decay, thus likely representing a null mutation. The nonsense mutation p.(Gln314*) in the last coding exon is predicted to lead to a truncated protein, lacking the last 63 C-terminal amino acids, which include the last WD40 repeat. All three amino acid residues affected by missense mutations are evolutionary highly conserved (Fig. 1C), and all three missense mutations are predicted to be damaging by multiple *in-silico* algorithms (Table 1). Structural modeling indicated that all three missense mutations would cause local steric hindrances within the WDR73 protein, which might result in destabilization or defective folding of the protein (Supp. Figures S1, S2). Of note, modeling of the N-terminal domain of WDR73 affected by the p.(Leu23Gln) and p.(Arg96Lys) mutations, upstream of the predicted 6 WD40 repeats, suggested that this domain might contain 2 helix-hairpin-helix (HhH) motifs. HhH motifs facilitate non-sequence-specific DNA binding, consistent with the cell cycle-dependent nuclear localization of WDR73 and its supposed function in microtubule-polymerization (Cui and Hawley, 2005; Cui et al., 2005; Colin et al., 2014).

Clinical features in patients with *WDR73* mutations

A summary of clinical findings in 10 affected individuals from 5 families harboring biallelic *WDR73* mutations is provided in Table 1, together with the clinical findings in the five previously reported individuals (Colin et al., 2014; Ben-Omran et al., 2015). Representative brain MRI pictures from patients II-1 and II-2 from family 1 are shown in Fig. 2. A detailed clinical description has been previously published for the five individuals affected by CAMOS/SCAR5 from family 2 (Megarbane et al., 2001) and for the index patient from family 4 (Steiss et al., 2005) (Table 1).

Cranial MRIs showed infantile-onset CA without brain stem involvement in all patients examined (Table 1) and variable basal ganglia degeneration and brain atrophy (Fig. 2). This was documented to be an early infantile onset neurodegenerative disease by serial imaging in patients from family 1 (Fig. 2). Patients presented with a progressive neurological phenotype of infantile-onset, and dystonia was a striking symptom already present in

infancy. While infantile-onset CA and ataxia, intellectual disability, visual impairment and secondary microcephaly were consistent findings in the majority of patients, renal involvement showed high inter- and intra-familial variability considering prevalence, age of onset, and type of kidney disease (Table 1). Onset of kidney involvement ranged from infantile (family 3) to late-adolescent, and also absence of renal involvement was documented in adults with homozygous *WDR73* mutations. When present, kidney involvement associated with *WDR73* mutations comprised a broad spectrum ranging from mild non-nephrotic proteinuria (family 1) to overt nephrotic syndrome with rapid progression to end-stage kidney disease (family 3). Ocular involvement included optic atrophy as a common finding. Oculomotor apraxia, strabismus and myopia were documented in the patient from family 5, and a retinopathy in both patients from family 1. Short stature was present in a majority of patients (Table 1). We observed a very slow proliferation rate of fibroblasts cultured from patients from family 1 (data not shown) as reported previously (Colin et al., 2014).

DISCUSSION

WDR73 deficiency was recently identified as a rare cause of GMS in five patients from five unrelated families (Colin et al., 2014; Ben-Omran et al., 2015). GMS is rare and characterized by nephrotic syndrome, usually of early onset, in association with microcephaly and variable brain abnormalities. Our study of large patient cohorts and the first description by Colin et al. (2014) indicate that it is a genetically heterogeneous disease. Overall, nephrotic syndrome most often develops within the first months of life in GMS and leads to death before the age of six years due to end-stage kidney disease (Galloway and Mowat, 1968; Steiss et al., 2005). However, a later onset of renal involvement was demonstrated in four out of five patients with WDR73 deficiency between five and twelve years of age (Colin et al., 2014; Ben-Omran et al., 2015). We expand the phenotypic and molecular spectrum of *WDR73*-related disease by describing 10 patients from five unrelated families with mutations in this gene. Our data show that biallelic *WDR73* mutations are rarely associated with the typical GMS phenotype, but rather present as an isolated infantile-onset neurodegenerative disease that may be followed by signs of a glomerulopathy manifesting between childhood and adolescence. GMS patients reported to carry *WDR73* mutations displayed a similar pattern of anomalies on neuroimaging with CA as a prominent finding (Colin et al., 2014).

In addition, we also revisit the molecular basis of CAMOS/SCAR5, by providing evidence that biallelic mutations in *WDR73* cause CAMOS/SCAR5. The CAMOS phenotype had been delineated in a large inbred Lebanese pedigree with congenital non-progressive spastic ataxia, microcephaly, optic atrophy, short stature, speech defect, cerebellar atrophy, and severe intellectual disability, as well as an abnormal osmiophilic pattern of skin vessels (Megarbane et al., 2001). Homozygosity mapping distinguished a novel locus for autosomal recessive cerebellar ataxia (SCAR5) in this family (Delague et al., 2002). Subsequently, sequencing of a number of selected candidate genes from the linkage region resulted in the identification of a homozygous missense variant in *ZNF592*, p.(Gly1046Arg), which was considered disease-causing at the time (Nicolas et al., 2010).

WDR73, albeit located within the linkage interval, had not been sequenced at that time because its function had been completely unknown. However, the *ZNF592* p.(Gly1046Arg) variant scores as benign by *in-silico* analyses (Poly-Phen benign, SIFT tolerated) in contrast to the p.(His347Tyr) mutation in *WDR73*. Moreover, *WDR73* mutation screening of our patient cohort with early-onset CA revealed one additional patient with a homozygous *WDR73* mutation (family 5), whereas no further *ZNF592* mutations were detected in our CA cohort. The causative role of mutations in this gene for a CA or CAMOS phenotype has not been replicated since its publication in 2010. However, we cannot exclude the possibility that the variation in *ZNF592* might have additive or modifying effects on the phenotype observed in the original CAMOS/SCAR5 family. Notably, an abnormal osmiophilic pattern of skin vessels was described in this family (Megarbané et al., 2001), while no such abnormalities were noted in both patients from family 1, suggesting that this is no characteristic feature of *WDR73*-associated disease. Nevertheless, since all the major neurological features observed in the original CAMOS/SCAR5 family are similar to the phenotypes observed in other individuals with *WDR73* mutations, we conclude that CAMOS/SCAR5 is part of the phenotypic spectrum of *WDR73*-associated disease.

With the first description of early infantile-onset of movement disorder and progressive basal ganglia degeneration, we also expand the neurological spectrum of *WDR73*-associated disease. Neurodegenerative movement disorders of infantile onset are both rare and genetically heterogeneous and occur in metabolic disorders and in inherited neurodegenerative diseases such as spinocerebellar ataxias (Reetz et al., 2013), and in neurodegeneration with brain iron accumulation (NBIA; MIM #300894) (Hayflick et al., 2013; Saitsu et al., 2013). While *WDR45* (MIM #300526) mutations cause basal ganglia degeneration with brain iron accumulation in NBIA, such an accumulation was excluded in cranial MRI in patient 1-II-1 with basal ganglia degeneration due to *WDR73* mutations. We further demonstrate postnatal onset of CA and progressive neurodegeneration by serial cranial MRIs in both patients from family 1 with *WDR73* mutations. This supports the hypothesis of an important role for WDR73 in neuronal cell survival in the cerebellum (Colin et al., 2014) and provides evidence for an important function also in basal ganglia cell survival. While gyral abnormalities have initially been considered as essential for making the diagnosis of GMS (Galloway and Mowat, 1968) neither the three reported WDR73-deficient patients (Colin et al., 2014) nor the patients reported here presented with cortical migration or gyration defects, whereas CA was the most prominent and a constant MRI feature. Based on the observations of a total of 15 patients (five previously reported ones and 10 described here), the typical neurological phenotype in *WDR73* mutations comprises secondary microcephaly, severe intellectual disability, visual impairment, and CA with variable basal ganglia involvement (Table 1).

Occurrence of retinopathy is another novel feature associated with *WDR73* mutations and has never been described in GMS. Diagnosis of retinopathy in GMS might have been missed previously as many patients die within the first years of life and as visual impairment might be considered as a consequence of optic atrophy, which is a common feature in GMS. Infantile onset of short stature as reported in the CAMOS/SCAR5 family was a common feature in other individuals with *WDR73* mutations suggesting that short stature is part of the

clinical phenotype caused by *WDR73* mutations. Factors contributing to short stature may represent the severe infantile feeding difficulties as well as a primary defect in cell survival and microtubule regulation that was described in fibroblasts from individuals with *WDR73*-associated disease (Colin et al., 2014).

Although renal involvement appears to be no constant feature in WDR73-associated disease, life expectancy seems to depend on the age of onset of glomerular kidney disease. Inter-familial variability in the onset of glomerular kidney disease might be explained by particular *WDR73* mutation type as indicated by five patients homozygous for p.(His347Tyr) without renal involvement at current ages between 25 and 31 years, or by other modifying effects. In contrast, family 3 with a different missense mutation p.(Arg96Lys) displayed severe and early-onset renal disease. Factors contributing to intra-familial variability particularly regarding the renal manifestations need to be identified.

In summary we describe 10 patients from five families with *WDR73* mutations, presenting with a predominantly infantile-onset neurodegenerative disease with CA, variable basal ganglia degeneration, intellectual disability and movement disorder. Results from the mutational survey indicate that biallelic mutations in *WDR73* may account for up to 6 % of CA with variable brain anomalies cases and 5 % of GMS cases in our cohorts. These results highlight *WDR73* as an important disease gene in infantile-onset neurodegeneration and CA.

Supplementary Material

Refer to Web version on PubMed Central for supplementary material.

Acknowledgments

This study was partially funded by the Austrian society of Pediatrics (ÖGKJ) and an in-house grant of the Department of Pediatrics and Adolescent Medicine of Medical University Vienna (to J.V.). This study was partly sponsored by the French Association against Myopathies “Association Française contre les Myopathies” (AFM), the “Agence Universitaire de la Francophonie” (AUF) and the European Union’s Seventh Framework Programme for research, technological development and demonstration under grant agreement n°294983 (LEB’IN project:Lebanon-Europe “on boarding” to innovate and enhance research links in health). Mirna Assoum was supported by a grant from the the Institut National de la Santé et de la Recherche Médicale (Inserm) and by the European Union (LEB’IN project: grant agreement n°294983). The authors declare no competing financial interests.

References

Abecasis GR, Cherny SS, Cookson WO, Cardon LR. Merlin--rapid analysis of dense genetic maps using sparse gene flow trees. Nat Genet. 2002; 30:97–101. [PubMed: 11731797]

Adzhubei IA, Schmidt S, Peshkin L, Ramensky VE, Gerasimova A, Bork P, Kondrashov AS, Sunyaev SR. A method and server for predicting damaging missense mutations. Nat Methods. 2010; 7:248–9. [PubMed: 20354512]

Ben-Omran T, Fahiminiya S, Sorfazlian N, Almuriekhi M, Nawaz Z, Nadaf J, Abu Khadija K, Zaineddin S, Kamel H, Majewski J, Tropepe V. Nonsense mutation in the WDR73 gene is associated with Galloway-Mowat syndrome. J Med Genet. 2015

Colin E, Huynh Cong E, Mollet G, Guichet A, Gribouval O, Arrondel C, Boyer O, Daniel L, Gubler MC, Ekinci Z, Tsimaratos M, Chabrol B, et al. Loss-of-function mutations in WDR73 are responsible for microcephaly and steroid-resistant nephrotic syndrome: Galloway-Mowat syndrome. Am J Hum Genet. 2014; 95:637–48. [PubMed: 25466283]

Cooperstone BG, Friedman A, Kaplan BS. Galloway-Mowat syndrome of abnormal gyral patterns and glomerulopathy. Am J Med Genet. 1993; 47:250–4. [PubMed: 8213914]

Cui W, Hawley RS. The HhH2/NDD domain of the Drosophila Nod chromokinesin-like protein is required for binding to chromosomes in the oocyte nucleus. Genetics. 2005; 171:1823–35. [PubMed: 16143607]

Cui W, Sproul LR, Gustafson SM, Matthies HJ, Gilbert SP, Hawley RS. Drosophila Nod protein binds preferentially to the plus ends of microtubules and promotes microtubule polymerization in vitro. Mol Biol Cell. 2005; 16:5400–9. [PubMed: 16148044]

Delague V, Bareil C, Bouvagnet P, Salem N, Chouery E, Loiselet J, Megarbane A, Claustres M. A new autosomal recessive non-progressive congenital cerebellar ataxia associated with mental retardation, optic atrophy, and skin abnormalities (CAMOS) maps to chromosome 15q24-q26 in a large consanguineous Lebanese Druze Family. Neurogenetics. 2002; 4:23–7. [PubMed: 12030328]

Dietrich A, Matejas V, Bitzan M, Hashmi S, Kiraly-Borri C, Lin SP, Mildenberger E, Hoppe B, Palm L, Shiihara T, Steiss JO, Tsai JD, et al. Analysis of genes encoding laminin beta2 and related proteins in patients with Galloway-Mowat syndrome. Pediatr Nephrol. 2008; 23:1779–86. [PubMed: 18594871]

Galloway WH, Mowat AP. Congenital microcephaly with hiatus hernia and nephrotic syndrome in two sibs. J Med Genet. 1968; 5:319–21. [PubMed: 5713646]

Hayflick SJ, Kruer MC, Gregory A, Haack TB, Kurian MA, Houlden HH, Anderson J, Boddaert N, Sanford L, Harik SI, Dandu VH, Nardocci N, et al. beta-Propeller protein-associated neurodegeneration: a new X-linked dominant disorder with brain iron accumulation. Brain. 2013; 136:1708–17. [PubMed: 23687123]

Li H, Durbin R. Fast and accurate short read alignment with Burrows-Wheeler transform. Bioinformatics. 2009; 25:1754–60. [PubMed: 19451168]

Megarbane A, Delague V, Ruchoux MM, Rizkallah E, Maurage CA, Viollet L, Rouaix-Emery N, Urtizberea A. New autosomal recessive cerebellar ataxia disorder in a large inbred Lebanese family. Am J Med Genet. 2001; 101:135–41. [PubMed: 11391656]

Ng PC, Henikoff S. Predicting deleterious amino acid substitutions. Genome Res. 2001; 11:863–74. [PubMed: 11337480]

Nicolas E, Poitelon Y, Chouery E, Salem N, Levy N, Megarbane A, Delague V. CAMOS, a nonprogressive, autosomal recessive, congenital cerebellar ataxia, is caused by a mutant zinc-finger protein, ZNF592. Eur J Hum Genet. 2010; 18:1107–13. [PubMed: 20531441]

Reetz K, Costa AS, Mirzazade S, Lehmann A, Juzek A, Rakowicz M, Boguslawska R, Schols L, Linnemann C, Mariotti C, Grisoli M, Durr A, et al. Genotype-specific patterns of atrophy progression are more sensitive than clinical decline in SCA1, SCA3 and SCA6. Brain. 2013; 136:905–17. [PubMed: 23423669]

Roy A, Kucukural A, Zhang Y. I-TASSER: a unified platform for automated protein structure and function prediction. Nat Protoc. 2010; 5:725–38. [PubMed: 20360767]

Saitsu H, Nishimura T, Muramatsu K, Kodera H, Kumada S, Sugai K, Kasai-Yoshida E, Sawaura N, Nishida H, Hoshino A, Ryujin F, Yoshioka S, et al. De novo mutations in the autophagy gene WDR45 cause static encephalopathy of childhood with neurodegeneration in adulthood. Nat Genet. 2013; 45:445–9. 449e1. [PubMed: 23435086]

Steiss JO, Gross S, Neubauer BA, Hahn A. Late-onset nephrotic syndrome and severe cerebellar atrophy in Galloway-Mowat syndrome. Neuropediatrics. 2005; 36:332–5. [PubMed: 16217710]

Stirnimann CU, Petsalaki E, Russell RB, Muller CW. WD40 proteins propel cellular networks. Trends Biochem Sci. 2010; 35:565–74. [PubMed: 20451393]

Wolf NI, Koenig M. Progressive cerebellar atrophy: hereditary ataxias and disorders with spinocerebellar degeneration. Handb Clin Neurol. 2013; 113:1869–78. [PubMed: 23622410]

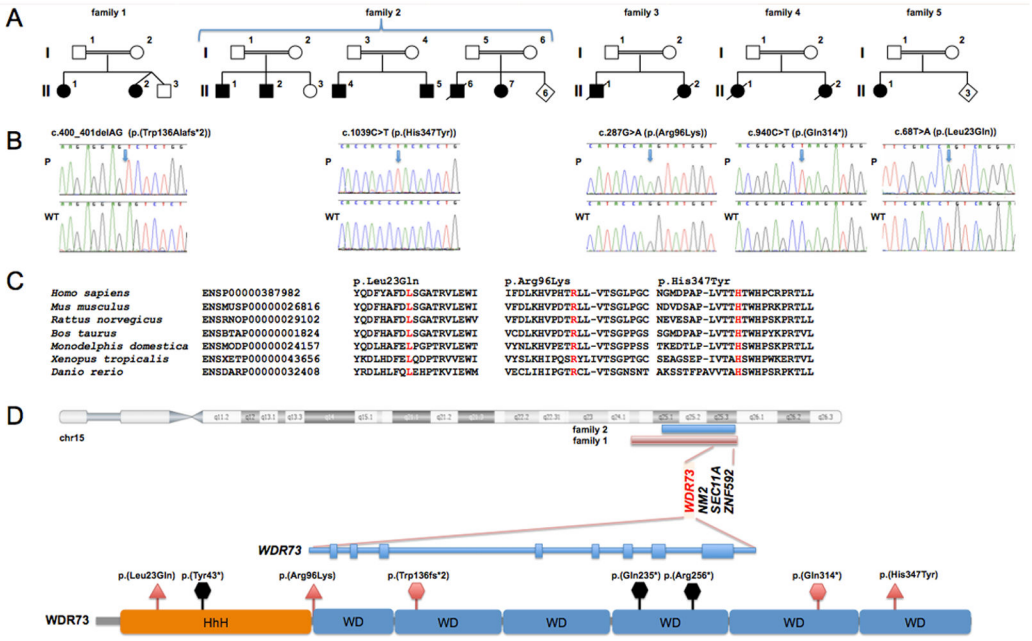

Figure 1.

Detection of *WDR73* mutations in five families. **A**, Simplified pedigrees of unrelated families segregating WDR73 mutations. All marriages with affected offspring were consanguineous. Note that affected individuals were present in three branches of family 2 (complete pedigree can be found in Nicolas et al., 2010). Individuals II-6 in family 2, II-1 in family 3, and II-1 in family 4 were reportedly affected, but neither sufficient clinical information nor DNA samples were available for confirmation of mutations and genotype-phenotype correlation analysis. **B**, Sequence chromatograms displaying homozygous mutations in affected patients (P) from each family compared with wild-type (WT). Nucleotide numbering uses +1 as the A of the ATG translation initiation codon in the reference sequence, with the initiation codon as codon 1. **C**, The three identified missense mutations affect invariantly conserved amino acids in WDR73 orthologues. **D**, Linkage intervals of family 1 and the reported linkage region for family 2 (Delague et al., 2002) on chromosome 15q show a shared interval harboring WDR73. Scheme of the WDR73 gene with exons displayed as blocks and of the WDR73 protein with predicted domains. Mutations identified by Colin *et al.* (2014), Ben-Omran *et al.* (2015) and in this study are indicated in black and red, respectively (triangles denote missense mutations, hexagons denote truncating mutations); all reported mutations were observed in homozygous state in patients.

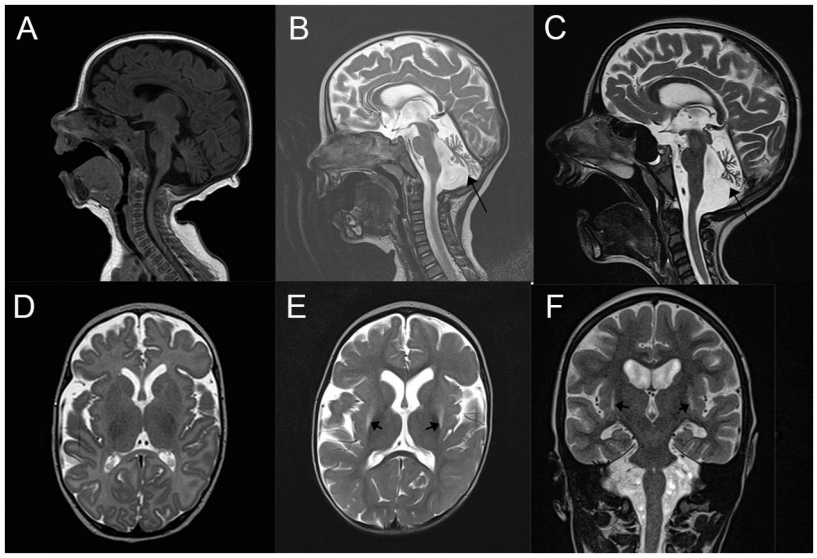

Figure 2.

Progressive cerebellar atrophy and basal ganglia involvement in two siblings homozygous for WDR73 mutation p.(Trp136fs2*). Serial brain MRIs show progression of cerebellar atrophy in patient II-2 from family 1: Brain MRI demonstrate mild enlargement of outer cerebrospinal fluid spaces and normal signal intensity of basal ganglia at three months of age (**A**, **D**), but displays severe cerebellar atrophy as indicated by an arrow in (B) and shows bilateral T2-weighed hyperintensities of putamina (arrows in **E**) at one year and four months of age. Most severe cerebellar atrophy as indicated by an arrow in (C) and T2-weighed hyperintensities of putamina as indicated by arrows in (F) are present in the affected sister (II-1) at 9.5 years of age.

Table 1

Clinical characteristics and neuroimaging in biallelic *WDR73* mutations

	Present study										Colin *et al.*			Ben-Omran *et al.*		Total
Individual	**1-II-1**	**1-II-2**	**2-II-1**	**2-II-2**	**2-II-4**	**2-II-5**	**2-II-7**	**3-II-1**	**4-II-1**	**5-II-1**	**A-II-3**	**A-II-4**	**B-II-3**	**1**	**2**	**15**
Sex	F	F	M	M	M	M	F	F	F	F	M	M	M	F	F	7 M / 8 F
Current age	11y	6y	27y	26y	31y	30y	25y	Died at 2.5y (ESRD)	Died at 17y (ESRD)	11y	Died at 5y (ESRD)	7y	13y	12y	5y	5–31 years, 3 deceased
Consanguinity	+		+					+	+	+	–		+	+	+	7/8 families
Ethnicity	Austrian		Lebanese					Indian	Turkish	Somalian	Moroccan		Turkish	Arab		divers
Original diagnosis	Syndromic CA		CAMOS, syndromic CA					GMS	GMS	CA	GMS		GMS	GMS		5 GMS, 3 CA
Neurological features																
Microcephaly (< 3rd centile)	+	+	+	+	+	+	+	+	+	–	+	+	+	–	–	13/15
Intellectual disability	Profound	Profound	Profound	Profound	Profound	Profound	Profound	Severe	Profound	Mild	+	+	+	Severe	+	15/15
Seizures	–	+	–	–	–	–	–	+	+	–	+	+	–	+	+	7/15
Axial hypotonia	+	+	–	–	–	–	+	+	+	+	+	+	+	+	+	11/15
Ataxia	+	+	+	–	–	–	–	ND	+	+	NR	NR	NR	NR	NR	5/14
Spasticity	–	–	+	+	+	+	+	–	–	+	–	–	+	+	+	9/15
Dystonia	+	+	+	–	+	+	–	+	+	+	–	–	–	–	–	8/15
Mobility	–	–	Crawling	Assisted walking	Assisted walking	Assisted walking	Assisted walking	–	sitting	Assisted walking	NR	NR	NR	sitting	–	Limited in 12/15
Speech	–	–	–	–	–	–	very few words	–	–	+	NR	NR	NR	–	–	Absent or limited in 11/12
Irregular sleep pattern	+	+	+	–	–	–	–	ND	+	–	NR	NR	NR	NR	NR	4/9
Feeding problems	+	+	+	–	–	–	–	+	+	+	NR	NR	NR	NR	NR	6/10
Brain imaging																
Cerebellar atrophy	+	+	+	ND	+	ND	+	ND	+	+	+	+	+	+	+	12/12
Neural migration defects	–	–	–	ND	–	ND	–	ND	–	–	–	–	–	–	–	0/12
Myelination defects	–	–	–	ND	–	ND	–	ND	–	+	–	–	–	+	+	3/12
Brain atrophy	+	+	–	ND	–	ND	–	ND	+	+	–	+	+	+	+	8/12
Basal ganglia degeneration	+	+	–	ND	–	ND	–	ND	–	–	–	–	–	–	–	2/12
Other imaging findings	Exclusion of metal deposits, normal spectroscopy	Normal fetal and neonatal MRI, normal spectroscopy									Thin corpus callosum		Thin corpus callosum	Dandy walker variant deformity, small brainstem, thin corpus callosum		
Eye symptoms																
Optic atrophy	+	+	+	+	+	+	+	ND	+	–	+	+	+	+	+	13/14
Retinopathy	+	+	–	–	ND	ND	–	ND	ND	–	NR	NR	NR	NR	NR	2/6
Renal involvement																
Proteinuria (age at detection)	–	5.5y[a]	–	–	ND	ND	ND	6m	16y	7y[b]	5y	–	–	12y	–	6/12

	Present study										Colin *et al.*			Ben-Omran *et al.*		Total
Individual	**1-II-1**	**1-II-2**	**2-II-1**	**2-II-2**	**2-II-4**	**2-II-5**	**2-II-7**	**3-II-1**	**4-II-1**	**5-II-1**	**A-II-3**	**A-II-4**	**B-II-3**	**1**	**2**	**15**
Without renal involvement	11y	–	27y	26y	31y	30Y	25Y	–	–			7y	13y	–	5y	9/15
Renal biopsy	ND	FSGS at 5.5y	ND	ND	ND	ND	ND	FSGS at 1.5y	FSGS at 16.5y	ND	collapsing FSGS, podocyte hypertrophy at 5y	Normal at 7y	FSGS, podocyte hypertrophy	ND	ND	
Miscellaneous																
Short stature SD	+ −3	+ −3	+ −5.5	+ −5.5	+ −4	+ −5	+ −3	ND	+ −2.5	–	NR	NR	NR	NR	NR	8/9
Other clinical features	strabismus	strabismus	strabismus	strabismus	strabismus	strabismus	Ptosis	Hearing loss	Hiatal hernia	Ptosis, myopia strabismus, oculomotor apraxia, facial muscles weakness, joint laxity	Facial dysmorphism	Facial dysmorphism	Facial dysmorphism	Facial dysmorphism, hypopigmentation of skin		
Genetics																
WDR73 Mutation[c]	c.400_401delAG p.(Trp136Alafs*2)		c.1039C>T p.(His347Tyr)					c.287G>A p.(Arg96Lys)	c.940C>T p.(Gln314*)	c.68T>A p.(Leu23Gln)	c.129T>G p.(Tyr43*)		c.766dupC p.(Arg256Profs*18)	c.703C>T p.(Gln235*)		15/15
Predicted mutation effect	Early truncation (136/377 aa) / NMD		Missense Highly conserved In WD40 domain					Missense Highly conserved	Truncated protein (last exon, 314/377 aa)	Missense Highly conserved	Early truncation (43/377 aa) / NMD Early truncation (43/377 aa) / NMD		Early truncation (256/377 aa) / NMD	Early truncation (235/377 aa) / NMD		
PolyPhen-2	NA		Probably damaging					Probably damaging	NA	Probably damaging	NA		NA	NA		
SIFT	NA		Not tolerated					Not tolerated	NA	Not tolerated	NA		NA	NA		
UMD	NA		Pathogenic					Pathogenic	NA	Pathogenic	NA		NA	NA		
ESP frequency	0		0					0	0	0	0		0	0		
EXAC frequency	1/120062		1/ 84686					0	0	0	0		0	0		
ZNF592 sequence analysis	No mutation	ND	c.3136G>A p.(Gly1046Arg)					No mutation	No mutation	No mutation	No mutation	ND	ND	ND		

+, present; −, absent; CA, cerebellar atrophy; GMS, Galloway-Mowat syndrome; ESRD, endstage renal disease; FSGS, focal segmental glomerulosclerosis; ND, not determined; NR, not reported; NA, not applicable

[a] proteinuria was detected during an episode of Purpura Schönlein-Henoch) and was persistent,

[b] proteinuria detected at screening for metabolic disorders; NMD, nonsense-mediated mRNA decay; aa, amino acid(s),

[c] National Center for Biotechnology Information (NCBI) reference sequence NM_032856.3